Reaction mechanisms of the $^{16}O + ^{65}Cu$ system

E. Crema,[1,*] V. A. B. Zagatto,[1,2] J. M. B. Shorto,[3] B. Paes,[2] J. Lubian,[2] R. F. Simões,[1] D. S. Monteiro,[4,5] J. F. P. Huiza,[6] N. Added,[1] M. C. Morais,[7] and P. R. S. Gomes[2,1]

[1]*Departamento de Física Nuclear, Instituto de Física da Universidade de São Paulo, Caixa Postal 66318, 05315-970 São Paulo, São Paulo, Brazil*

[2]*Instituto de Física, Universidade Federal Fluminense, Avenida Litorânea s/n, Gragoatá, Niterói, Rio de Janeiro, 24210-340, Brazil*

[3]*Instituto de Pesquisas Energéticas e Nucleares, IPEN/CNEN, 05508-000 São Paulo, São Paulo, Brazil*

[4]*ILACVN, Universidade Federal da Integração Latino-Americana, 85866-000 Foz do Iguaçu, Paraná, Brazil*

[5]*Department of Physics, University of Notre Dame, South Bend, Indiana 46556, USA*

[6]*Universidade Estadual do Sudoeste da Bahia, Bahia, Brazil*

[7]*INFES, Universidade Federal Fluminense, Santo Antonio de Pádua, 28470 000 Rio de Janeiro, Brazil*

(Received 11 December 2018; published 24 May 2019)

We have measured a precise quasielastic excitation function for the $^{16}O + ^{65}Cu$ system, at $\theta_{LAB} = 161^{\circ}$, and at bombarding energies near the Coulomb barrier. A quasielastic barrier distribution for this system was deduced from the experimental quasielastic excitation function. An α-stripping excitation function has also been measured at the same experimental conditions. These new data have been used to investigate the relative importance of several reaction channels in the reaction mechanism of the $^{16}O + ^{65}Cu$ system. Large-scale coupled-channel calculations and coupled-reaction-channel calculations have been performed. No imaginary potential was used at the barrier region because many channels have been explicitly included in the calculations. Only an inner short-range potential was used to account for the fusion process. We did not fit data by varying potential parameters, and our theoretical results were compared directly to data. Good agreement was found between data and calculations. Owing to the high sensitivity of the barrier distribution, important results have been obtained. The first excited state $(1/2^-)$ of ^{65}Cu has less influence in the reaction mechanism than the second $(5/2^-)$ and third $(7/2^-)$ states, which are the most relevant among all the investigated ones. We have also observed a striking influence of the reorientation of the ground-state spin of the ^{65}Cu nucleus on the elastic scattering at backward angles. In addition, calculations have shown that the excitation of the states 3^-, 2^+, 1^-, and 2^- of the projectile ^{16}O are also important for excellent agreement obtained with both the excitation function and the distribution of barriers. The α-stripping data have been compared to the results of coupled-reaction-channel calculations and good agreement was obtained with the inclusion of the first excited state of ^{12}C in the coupling scheme. However, the α-transfer process has a small influence on the reaction dynamics of this system at the investigated energies.

DOI: 10.1103/PhysRevC.99.054623

I. INTRODUCTION

The reaction dynamics of heavy nuclei collisions at bombarding energies near the Coulomb barrier is governed by a delicate quantum interference of all reaction channels. As nuclear structures of the interacting nuclei strongly affect this quantum process, it is important to perform systematic studies to identify which are the most relevant channels in each system [1–7]. Disentangling the individual role of each channel in this process is important for both reaction mechanism studies and nuclear structure investigations. However, this is a difficult task from both experimental and theoretical points of view, because a high number of channels might be involved. Experimentally, many reaction channels should be measured, and it could be difficult (or even impossible) to kinematically separate each channel. However, the development of barrier distribution methods made this task easier because one needs to measure only inclusive data instead of a large number of excitation functions [8–14]. Owing to the high sensibility of the barrier distribution, one can investigate the relative role of each channel on the reaction mechanism.

At energies around the Coulomb barrier, the quasielastic process is defined as the sum of elastic, inelastic, and transfer reactions. From a single high-precision quasielastic excitation function (EF), taken at backward angles, one can deduce the corresponding quasielastic barrier distribution (QEBD) from the mathematical operation [10]:

$$D^{\rm qel}(E) = -\frac{d}{dE}\left[\frac{d\sigma^{\rm qel}(E)}{d\sigma^{\rm Ruth}(E)}\right]. \quad (1)$$

On the other hand, from a theoretical point of view, the difficulties of closely studing a reaction mechanism of collisions between heavy nuclei in a more fundamental way are the following: the large number of channels that must

*crema@if.usp.br

 ©2019 American Physical Society

be taken into account in the coupled-channels calculations, the lack of experimental nuclear parameters for the higher excited states of most of the nuclei, and the correct choice of nuclear potentials to describe the interaction between the nuclei. In addition, as Satchler pointed out several years ago, when a deformed odd nucleus is involved in the reaction, an interesting phenomenon can occur due to the nonzero spin and the ground-state static deformation of this nucleus: the reorientation of its ground-state spin [15,16]. Since then, phenomena related to ground-state nuclear spin and nuclear deformation of target and/or projectile have been largely investigated [17–21].

We have previously studied the $^{16,18}\mathrm{O} + {}^{63}\mathrm{Cu}$ systems and, indeed, the reorientation effect had a strong influence on their reaction mechanisms [22,23]. So, to continue building a systematic study in this odd-mass nuclei region, we decided to study the $^{16}\mathrm{O} + {}^{65}\mathrm{Cu}$ system, because the $^{65}\mathrm{Cu}$ has the ground-state spin $3/2^-$ and the large ground-state quadrupole moment, $Q = -0.195$ b. To overcome the first difficulty pointed out above, we performed large coupled-channel calculations (CCC) and coupled-reaction-channel (CRC) calculations that include, besides the reorientation mechanism, many inelastic channels and the α-stripping reaction, to investigate their relative role in the reaction dynamics. The aims of accounting for a lot of channels were not only to learn about them but also to avoid using arbitrary imaginary potentials to describe the global effect of these channels. So, we do not need to employ an imaginary potential at the barrier region to describe the flux absorption by the reaction channels because we have included explicitly as many channels as possible in the coupling matrix. To account for the fusion process, we simulate the incoming wave boundary condition by using an inner short-range imaginary potential, which has a negligible influence on the direct process results. On the other hand, for the real nuclear potentials that describe the interaction between the colliding nuclei, we used the double-folding Sao Paulo potential (SPP), which is parameter free in the sense that it is constructed with average nuclear (matter and charge) parameters obtained from large systematic studies [24,25]. So, the main features of our theoretical approach are that we are not interested in fitting data by varying potential parameters and the results of our calculations are directly compared to data. Thus, one by one, all inelastic excitations, for which there are experimental $B(E2)$ in the literature, are included in the CCCs.

In previous work, we have found an important contribution of the α-stripping process in the $^{16}\mathrm{O} + {}^{63}\mathrm{Cu}$ system, which put in evidence, once more, the α-cluster structure of the $^{16}\mathrm{O}$ nucleus, because all the other few-nucleon transfers had much lower cross sections than the α transfer at the same experimental conditions. So, in the present paper, we decided to investigate how the neutron occupancy of the $f_{7/2}$ neutron subshell of the copper isotopes can affect the α-stripping process. Thus, we measured and compared it in both $^{16}\mathrm{O} + {}^{63}\mathrm{Cu}$ and $^{16}\mathrm{O} + {}^{65}\mathrm{Cu}$ systems. Large CRC calculations were employed to investigate this transfer channel, including several excited states of the nuclei in both entrance and exit channels. Beside it, we have measured a high-precision quasielastic EF, from which its correspondent QEBD was

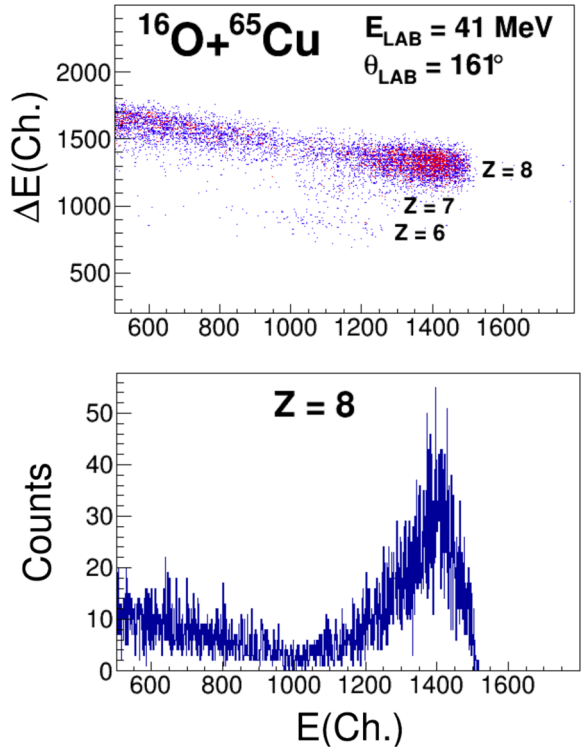


FIG. 1. (a) $E - \Delta E$ spectrum of the $^{16}\mathrm{O} + {}^{65}\mathrm{Cu}$ system taken at $E_{\mathrm{LAB}} = 41$ MeV and $\theta_{\mathrm{LAB}} = 161^\circ$ and (b) energy spectrum of the events with $Z = 8$ of the $E - \Delta E$ spectrum above.

derived. In addition to these new data, our analysis includes an elastic scattering angular distribution for the $^{16}\mathrm{O} + {}^{65}\mathrm{Cu}$ system, taken at $E_{\mathrm{LAB}} = 46.5$ MeV, that were available but not published yet [26].

In Sec. II, we describe the experiment and present the results, which are compared to the data from neighboring systems, $^{16}\mathrm{O} + {}^{63}\mathrm{Cu}$ and $^{18}\mathrm{O} + {}^{63}\mathrm{Cu}$. In Sec. III, the CCC and CRC calculations are described and their results discussed. Finally, we summarize our results and present our conclusions.

II. EXPERIMENT AND RESULTS

Measurements were made at the São Paulo University Pelletron Accelerator Facility, where its 8UD tandem electrostatic accelerator has delivered beams of $^{16}\mathrm{O}$ with intensities ranging from 10 to 80 pnA, in the energy range of 30.0–48.0 MeV, and with energy steps of 0.5 MeV. The beams were incident on a self-supporting target of thickness 70 μg/cm^2 of isotopically enriched $^{65}\mathrm{Cu}$ (99.01%).

The projectile-like fragments (PLFs) were detected by a $E - \Delta E$ proportional telescope, placed at $\theta_{\mathrm{LAB}} = 161^\circ$, where ΔE is the energy lost by the scattered ion in a volume of the gas mixture P-10, at a pressure of 20 torr. On the other hand, the residual energies of the PLF's, E, were measured by a silicon surface barrier detector placed behind the gas volume. An $E - \Delta E$ spectrum, taken at $E_{\mathrm{LAB}} = 41$ MeV, is shown in Fig. 1(a), where one can see that the resolution in Z is good enough to identify PLFs with $Z = 6, 7, 8$ in the energy region of interest. Figure 1(b) presents the energy spectrum

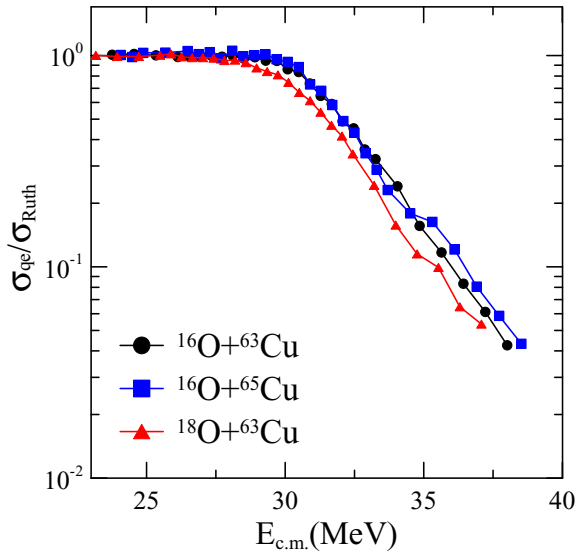


FIG. 2. Excitation functions measured at $\theta_{LAB} = 161^\circ$ for the systems $^{16}O + ^{65}Cu$ (present work) and $^{16,18}O + ^{63}Cu$ from Refs. [22,23].

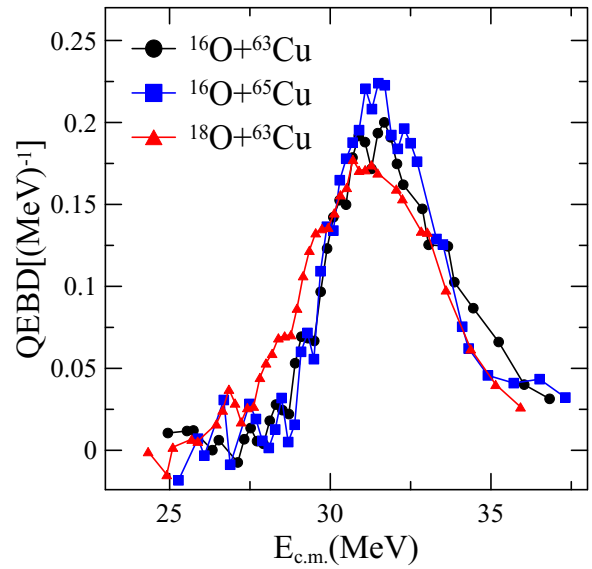


FIG. 3. Quasielastic barrier distributions measured at $\theta_{LAB} = 161^\circ$ for the systems $^{16}O + ^{65}Cu$ (present work) and $^{16,18}O + ^{63}Cu$ from Refs. [22,23].

of all events with $Z = 8$, where one can see that the events coming from quasielastic processes are well identified. This figure also shows the presence of a background of events with $Z = 8$ that were produced by the scattering of the beam in the collimators, which, however, do not disturb the identification of the events of interest. The percentage of these spurious events that overlap with the quasielastic events was evaluated as being less than 3% for all energies, and they were properly subtracted. It should be emphasized that the experimental setup (solid angles, etc.) of this work was established only for the inclusive measurement of the quasielastic processes; that is, we were interested only in the measurement of several high-precision quasielastic cross sections in reasonable machine time. The experiment was not planned to identify and measure inelastic and transfer channels individually.

The quasielastic yields from the $E - \Delta E$ telescope were normalized by Rutherford scattering events taken by two silicon detectors placed at forwarding angles ($+30^\circ$ and -45°). The quasielastic EFs obtained by these two different normalizations were equal to each other inside the experimental uncertainties. The uncertainties of the measured EFs are lower than 1% for most of the energies and approximately 3% for some of the highest ones. The quasielastic EF measured for the system $^{16}O + ^{65}Cu$ is shown in Fig. 2, where two other neighboring systems that we have studied previously, $^{16,18}O + ^{63}Cu$, are also plotted [22,23]. As can be seen, the EFs of the three systems are similar. These EFs are not perfectly smooth at energies above the Coulomb barrier, where all of them present a small bump structure at different energies.

In the system under investigation, $^{16}O + ^{65}Cu$, its bump structure occurs at energies around 35 MeV, and it is a little more pronounced than in the other systems. In the case of the $^{16}O + ^{63}Cu$ system, a small structure appears at 33 MeV, approximately, while in $^{18}O + ^{63}Cu$, at energies around 34 MeV. If these structures are difficult to visualize in the excitation functions, the same does not occur in the barrier distributions. All experimental QEBDs discussed below were deduced from the measured quasielastic EF by means of a point-difference approximation with laboratory energy steps of 2.0 MeV, and all theoretical barrier distributions calculated in the next sections were deduced using the same procedure and energy steps. Figure 3 shows a comparison of the experimental QEBD of the three systems discussed above, where one can observe that they have different distributions. Error bars were omitted in this figure to facilitate comparison between systems, but they will be presented in later figures. It is interesting to note that the projectile ^{18}O has a strong effect on the reaction mechanism of the $^{18}O + ^{63}Cu$ system since it is responsible for producing QEBDs that are quite different from those of the other two systems. In fact, as proved in Ref. [23], the excitation of the ^{18}O is very important for the good agreement obtained between the theoretical calculations with both the experimental EF and the experimental QEDB of that system. It was proved that the first quadrupole excitation of the ^{18}O is the most important channel to explain the behavior of the EF at energies above the Coulomb barrier in the $^{18}O + ^{63}Cu$ system, including the structure discussed above. Therefore, this is a strong indication for the following investigation into the origin of this structure in the $^{16}O + ^{65}Cu$ system. So, it would be interesting to investigate more deeply the role of the projectile ^{16}O in the reaction mechanism.

III. THEORETICAL ANALYSIS

As commented before, the theoretical analysis of this paper is based on CCC and CRC calculations, and, as is well known, these procedures are strongly dependent on the nuclear potentials employed. Particularly in our theoretical approach, the choice of potentials is even more crucial, because we are interested in more fundamental parameter-free calculations.

We have already demonstrated that double-folding potentials are reliable bare potentials for describing reactions involving both stable and unstable nuclei [27–29]. So, in the present paper, the real nuclear interaction in the entrance channel was described by the real component of the double-folding São Paulo potential (SPP) [24,25], which is parameter free in the sense discussed before. It should be emphasized that no surface imaginary potential was used. On the other hand, the reaction flux that goes to the fusion process was accounted for by a short-range and fixed imaginary potential: $V_i = 80\,\text{MeV}$, $r_i = 0.8\,\text{fm}$, and $a_i = 0.6\,\text{fm}$, as suggested by Ref. [30]. This imaginary potential is a way to simulate the incoming wave boundary condition, and its geometry is such that it does not disturb the competition between the superficial channels. All the reported calculations have been performed using the FRESCO code [31].

In Sec. III A, the effect of each inelastic channel of the target (including the ground-state reorientation effect) will be presented. The inelastic channels of the projectile will be investigated in Sec. III B. The results of α-stripping transfer reactions are presented in Sec. III C. In Sec. III D, the calculations (and comparison to data) of the elastic angular distribution of $^{16}\text{O} + {}^{65}\text{Cu}$ system taken at bombarding energy of $E_{\text{LAB}} = 46.5\,\text{MeV}$ are presented.

A. Inelastic channels of the target ^{65}Cu

The coupled-channel study of the $^{16}\text{O} + {}^{65}\text{Cu}$ system aims to analyze the influence of each inelastic channel on the reaction mechanism by comparing theoretical results to the experimental quasielastic EF and its corresponding QEBD. So, the channels investigated will be included one at a time in the calculations, and the results will be presented as the cumulative effect of adding each one in the coupling scheme. The excited states of the ^{65}Cu which have been taken into account in the calculations were the following: $3/2^-$(g.s.), $1/2^-$ ($E^* = 0.77\,\text{MeV}$), $5/2^-$ ($E^* = 1.12\,\text{MeV}$), $7/2^-$ ($E^* = 1.48\,\text{MeV}$), $5/2^-$ ($E^* = 1.62\,\text{MeV}$), and $3/2^-$ ($E^* = 1.73\,\text{MeV}$).

The experimental $B(E2)\uparrow$ reduced transition probabilities of all of the couplings considered in the calculations have been taken from Ref. [32], which are all experimental $B(E2)\uparrow$ values available in the literature for the ^{65}Cu nucleus. However, for the highest bombarding energy of this work, almost 7 MeV above the Coulomb barrier, the available energy in the system can excite higher states of the target, which will not be included in the coupling matrix. This lack of basic nuclear data, even for stable nuclei, is a strong limitation for more fundamental theoretical analysis. The quadrupole moment, necessary to calculate the reorientation effect of the target's ground state, was taken from Ref. [33]. The adopted reduced matrix elements and the deformation lengths of each transition used in the calculations are listed in Table I.

The solid red lines in Fig. 4 represent the results of the CCC without any couplings, where Fig. 4(a) is the quasielastic EF and Fig. 4(b) is the QEBD. As can be seen in the figure, at energies below $E_{\text{c.m.}} = 30.0\,\text{MeV}$ both the experimental EF and QEBD are well explained by this simple uncoupled calculation, which indicates that the potential used describes quite well the bare interaction between projectile and target.

TABLE I. Table of the inelastic transitions of ^{65}Cu nucleus included in CC calculations. The transition to each final state (spin parity) are followed by the information of their respective energy transition, the reduced matrix element, and the deformation length. The $B(E\lambda)$ values were taken from Refs. [32] and [33].

^{65}Cu	Energy (MeV)	$\langle I_f \lvert E\lambda \rvert I_i\rangle$ e^2 fm^4	δ (fm)
$3/2^-$	Reor.	27.5	0.93
$1/2^-$	0.77	19.6	0.66
$5/2^-$	1.12	34.1	1.15
$7/2^-$	1.48	38.5	1.30
$5/2^-$	1.62	9.3	0.31
$3/2^-$	1.73	5.2	0.17

Besides, this agreement shows that below the Coulomb barrier ($V_B = 31.5\,\text{MeV}$) the reaction mechanism is dominated by the elastic scattering. However, above $E_{\text{c.m.}} = 30.0\,\text{MeV}$, both the EF and the QEBD show that the agreement between the

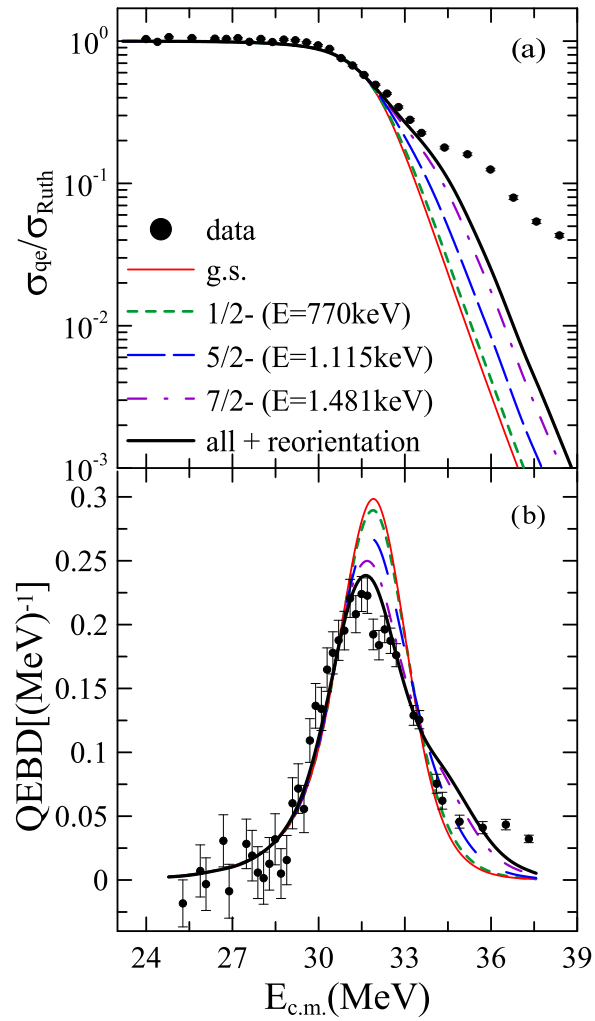


FIG. 4. (a) Experimental quasielastic excitation function, at $\theta_{\text{LAB}} = 161^\circ$, of the $^{16}\text{O} + {}^{65}\text{Cu}$ system and (b) its corresponding quasielastic barrier distribution. The curves are the results of the coupled-channel calculations discussed in the text.

uncoupled calculation and data became worse, which suggests that reaction channels are opened in this energy region. It is interesting to notice that the QEBD in Fig. 4(b) shows that inelastic channels are excited even for bombarding energies below the Coulomb barrier, which confirms the quantum character of these processes.

The first inelastic channel included in the calculation was the first excited state of the target, $1/2^-$ ($E = 0.77$ MeV), and its result is shown by the dashed green lines in Fig. 4, where a small improvement is observed in the agreement with data in both the EF and QEBD. The next step was to include in the coupling matrix, one by one, the other excited states of the target for which there are experimental reduced matrix elements available in the literature. The large-dashed cyan lines in Fig. 4 represent the result of the calculation that couples the first and the second excited states of the ^{65}Cu nucleus, and the dash-dotted magenta lines show the result of coupling its first three states shown in Table I. One can see clearly in the EF, and in the QEBD as well, that the $5/2^-$ and $7/2^-$ states have a strong influence in the quantum distribution of the total reaction flux. In fact, they are the most relevant states in the reaction mechanism among the target excited states investigated. The last two excited states presented in Table I were included in the calculation, but as they have a very small effect in the final results, they were not plotted in Fig. 4. One should notice that in the calculations shown in this figure, only the transitions between the excited states and the ground state were considered, disregarding the possible couplings between these excited states. Nevertheless, additional calculations considering all possible transitions between excited states were performed. Their inclusion did not affect significantly the EF and the QEBD.

On the other hand, the reorientation effect of the ground state of the target has also been included in the coupling matrix, and a striking influence on the reaction dynamics was observed. This effect can be seen in Fig. 4, where the black solid lines show that the reorientation channel is very important in both the EF and QEBD, at energies around and above the Coulomb barrier. A significant effect of the reorientation of the ground state of the neighboring nucleus ^{63}Cu has also been reported in Ref. [22], which was recently confirmed in Ref. [23].

Finally, according to the results of our previous works [22,23], if we compare the effects of the three most important channels of nuclei ^{63}Cu and ^{65}Cu ($1/2^-$, $5/2^-$, and $7/2^-$) in the reactions involving the same projectile ^{16}O, we notice that they have very similar behaviors, in spite of the different numbers of neutrons in the targets. On the other hand, if we consider the target ^{63}Cu bombarded by two different projectiles, ^{16}O and ^{18}O, the relative importance in the reaction mechanism of those three channels also remains approximately the same. Therefore, the excitation of the $1/2^-$, $5/2^-$, and $7/2^-$ states of nuclei ^{63}Cu and ^{65}Cu are approximately independent of the projectiles used in these studies, which is consistent with the fact that the respective transitions considered in these nuclei have similar reduced matrix elements.

Figure 4 shows that in the energy region 2.0 MeV above the Coulomb barrier, approximately, our theoretical description of the EF is poor, despite the reasonable agreement obtained for the QEBD. However, the same figure also presents a very important result: As more inelastic channels are included in the calculation, the more the theoretical curve evolves toward the data. It should be remembered that the highest excited state included in our calculations has only 1.73 MeV of energy. So, one of the possible explanations for this disagreement may be the lack of the several inelastic transitions that were not included in the coupling matrix, because they do not have reduced matrix elements available in the literature. Another possible explanation for this disagreement is the projectile excitation and the transfer channels, which will be discussed in the next subsections.

B. Inelastic channels of the projectile ^{16}O

Most theoretical works in the literature investigating the effects of ^{16}O excitation on reaction mechanisms only analyze its strong octupolar vibration (3^-, 6.1 MeV), and sometimes the quadrupolar vibration 2^+ at 6.9 MeV is also considered. So, as a first step, we included these two states in our calcu-

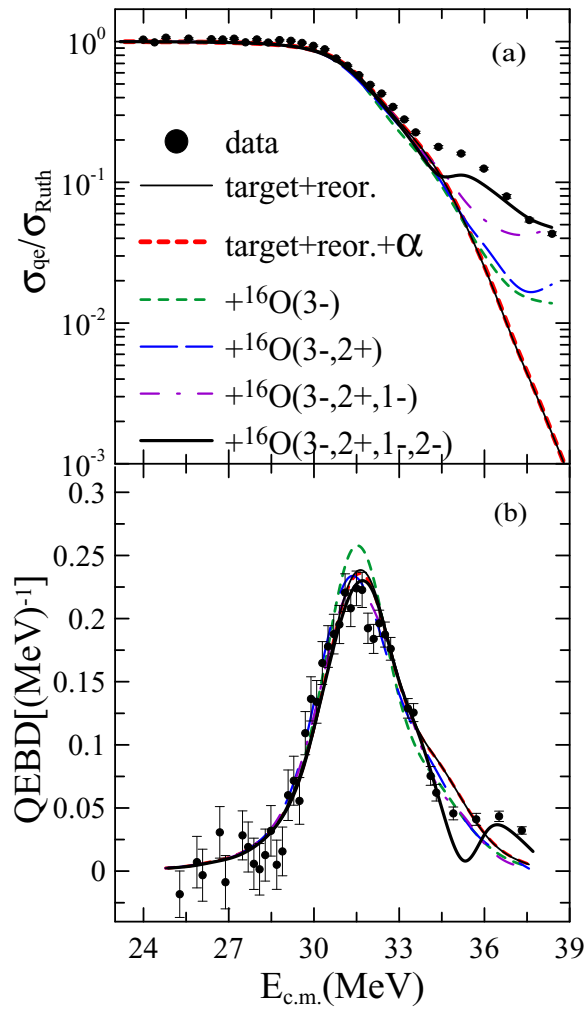


FIG. 5. (a) Experimental quasielastic excitation function, at $\theta_{LAB} = 161^\circ$, of the $^{16}O + ^{65}Cu$ system and (b) its corresponding quasielastic barrier distribution. The curves are the results of the coupled-channel calculations discussed in the text.

TABLE II. Table of the inelastic transitions of ^{16}O nucleus included in CC calculations. The information of each transition is followed of their respective reduced matrix element and the deformation length. The $B(E\lambda)$ values were taken from Refs. [34] and [35].

Initial	Final	$\langle I_f \|E\lambda\| I_i\rangle$ e^2 fm$^{2\lambda}$	δ (fm)
0^+	3^-	29.5	1.3
0^+	2^+	6.4	1.2
1^-	3^-	12.3	2.4
2^-	3^-	9.9	1.9
2^-	1^-	11.1	2.1

lations, and the results are shown in Fig. 5, where the lines represent the following: the dashed red line is the result of coupling all target states (presented before) and the α-transfer channel that will be discussed later; the dashed green line is the inclusion in the previous calculation of the ^{16}O(3^-) state; and the dashed blue line is the inclusion of the ^{16}O(2^+) state. The adopted reduced matrix elements and the deformation lengths of each transition used in the calculations are listed in Table II. The dashed blue line in Fig. 5(a) shows that they improve the agreement with the experimental EF.

However, analyzing the oxygen spectrum, we noticed that there are two other states that could be included in the coupling scheme: 1^- at 7.1 MeV and 2^- at 8.9 MeV. So, we decided to investigate these two channels that are not usually considered in the calculations. The results of the calculations including these states, one at a time, are very interesting and are represented in Fig. 5(a) by the dash-dotted magenta and solid black lines, respectively. While the 1^- state enhances the cross section at higher energy region toward the data, the 2^- state produces a striking agreement between the theoretical result and the experimental data. One possible explanation for this effect would be the fact that the decays of these two states have the 3^- as an intermediate state, as can be seen in Table II. We observed that the theoretical cross section of the 3^- state is largely increased by the opening of the 1^- and 2^- states.

Besides the very good accordance with the experimental EF obtained by our calculation, Fig. 5(b) reveals a striking result also for the QEBD. The CCC, including the projectile channels discussed before, improves the agreement between the theoretical QEBD and the experimental QEBD in the entire energy range investigated. It is interesting to note that, relative to the result obtained previously with the target states, the inclusion of only the 3^- state worsens the accordance with the QEBD in the region of the main peak, as shown by the dashed green line in Fig. 5(b). On the other hand, the dashed blue line shows that if the 2^+ state is added in the calculation together with the 3^- state, an improvement of the agreement occurs in the region of the main peak of the QEBD. It is also interesting to observe that, according to the dash-dotted violet line, the 1^- state produces a large effect on the EF, but in the QEBD its inclusion in the calculation practically does not change the previous result. However, among the excited states of the projectile, the 2^- state is the most decisive for achieving the excellent agreement reached by the CCC with both the experimental EF and QEBD. As shown by the solid black lines in Fig. 5, even the small peak observed at approximately 36 MeV in the QEBD is well described by the calculation.

Because of this important result for the system ^{16}O + ^{65}Cu, we also investigated whether the same effect also occurs in the ^{16}O + ^{63}Cu system. The results were similar, and its small structure in the EF at energies above the Coulomb barrier is also well explained when the four excited states of the ^{16}O discussed before are included in the CCC.

C. The α-transfer channel

The spectrum showed in Fig. 1 reveals that there are events coming from some transfer reactions, but the more relevant of them are those populating the region of the projectile-like fragment events with $Z = 6$, which will be considered as α-stripping processes. This is in accordance with the results of the Ref. [36], where it was observed that for the projectile ^{16}O, at low energies and relatively large internuclear separation, the α-stripping reaction dominates largely over the other transfer reactions. All the Q_{gg} values of the transfer reactions for the ^{16}O + ^{65}Cu system are largely negative. One of the less negative is the α stripping ($Q_{gg} = -2.67$ MeV), for which we have measured its excitation function, at $\theta_{\rm LAB} = 161^\circ$. Figure 7 shows the α-stripping cross sections divided by the correspondent Rutherford cross sections. For comparison, the same figure also plots the α-stripping excitation function for the neighboring system ^{16}O + ^{63}Cu that was studied in our previous work [22]. We can see that the maximum cross sections have similar values within the experimental uncertainties. However, the presence of two more neutrons in the $f_{7/2}$ neutron subshell of the nucleus ^{65}Cu seems to facilitate the α-stripping process at energies below the barrier. In the experimental spectra, there are also some stripping events with $\Delta Z = 1$, but the amount of counts is low, and their possible Q_{gg} values are very negatives. So, the α stripping is the only transfer channel that will be investigated.

In this section, CRC calculations will be employed to analyze the α-stripping reaction in the studied system. In these calculations, all the inelastic channels discussed in the previous section will also be coupled. Because of the significant amount of mass transferred from the incident ^{16}O during the α-stripping reaction (25%), it is not possible to use Brink's rule [37] to estimate the expected Q optimum value and the excitation energy of the recoiling nucleus. A first trivial attempt to infer the excited states of the resulting ^{69}Ga nucleus was done by adding to the coupling scheme all of its known states up to an energy of 1.7 MeV. The adopted coupling scheme in the CRC calculations is sketched in Fig. 6. The couplings considered only the ground state of the target in the initial partition because it is expected that the overlaps considering excitations in the initial ^{65}Cu would represent second-order transitions. Additional calculations (not shown here) showed that this is true.

The optical potential of the entrance partition was the same one used in our CCC of the previous section, where the inelastic excitations of the target were considered. In the outgoing partition, the São Paulo potential was used for both real and imaginary parts of the nuclear optical potential, with

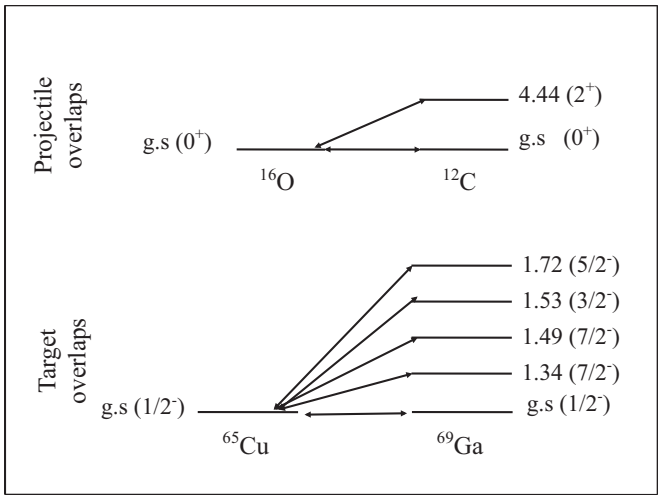


FIG. 6. Schematic representation of the CRC couplings. The lines represent the couplings between ground states of the initial partition (^{16}O and ^{65}Cu) to the states of the final partition (^{12}C and ^{69}Ga). The values of the excited-state energies are given in MeV.

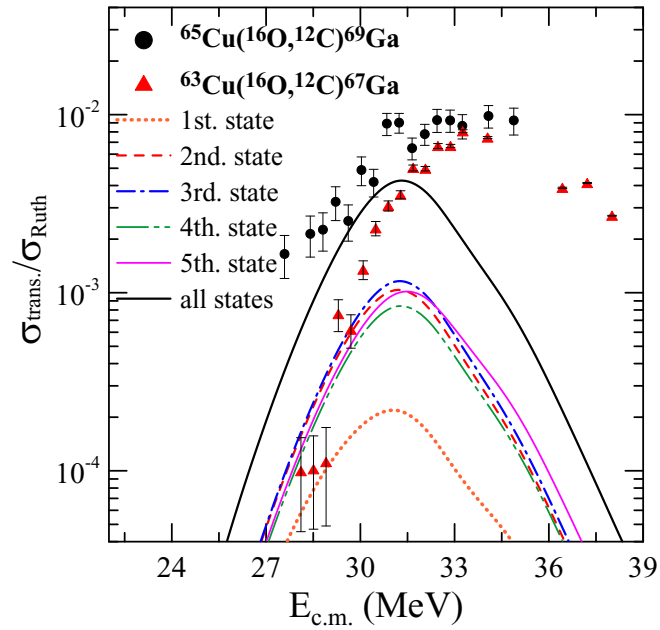


FIG. 7. Experimental data and different theoretical calculations of the excitation function for the $^{16}O(^{65}Cu, ^{69}Ga)^{12}C$ reaction. The data for the $^{16}O(^{63}Cu, ^{67}Ga)^{12}C$ reaction are plotted for comparison, and they were extracted from Ref. [22]. The lines are discussed in the text.

strength equal to $N_R = 1.0$ and $N_I = 0.78$, respectively. This normalization procedure was shown to be able to describe the elastic scattering of many systems in a wide mass and energy range [25]. The interactions of the valence α particle with the ^{12}C and ^{65}Cu cores were described by a Woods-Saxon potential with reduced radius $r_0 = 1.25$ fm and diffuseness $a = 0.75$ fm [23,38]. The depth of this central Woods-Saxon interactions was adjusted to reproduce the respective experimental binding energies in each case, $\alpha + ^{12}C$ and $\alpha + ^{65}Cu$. A complex remnant was adopted in the coupling matrix elements.

The same spectroscopic amplitude was assumed for all the possible target-recoil overlaps. In Ref. [39], the spectroscopic amplitude equal to 0.48 was proposed for the ground-to-ground $\langle ^{16}O|^{12}C\rangle$ overlap. This value is consistent with the one (0.51) obtained later in Ref. [40]. In all the overlaps, the valence α particle was treated in the extreme cluster configuration, with zero spin. The adjusted spectroscopic amplitudes for the target overlaps were equal to 0.3 in the present work, not very different from those obtained previously in the same context for the $\langle ^{67}Ga|^{63}Cu\rangle$ case [23]. The transfer cross sections resulting from these calculations, which include all the excited states of the ^{69}Ga nucleus indicated in Fig. 6, are compared with the data in Fig. 7. The solid black line in this figure represents the complete CRC calculation (including the inelastic channels), and the other lines are the individual contributions of each ^{69}Ga excited states to the total result. From Fig. 7, one can also see that all the states included in the CRC calculations have a similar shape and maximum at the same energy, approximately. Additional calculations revealed that the excitation functions of higher excited states of ^{69}Ga nucleus have the same shape and the maximum peak at the same energy region. It is also interesting to observe in this figure that experimental data points are almost constant for energies above $E_{c.m.} = 33$ MeV. However, the theoretical excitation functions for all states considered decrease above this energy. This may indicate that there are some missing channels that should be considered.

Indeed, the analysis of the experimental spectra reveals that the events with $Z = 6$ could correspond to reactions that let the ^{69}Ga and/or ^{12}C with excitation energies up to 5 MeV, approximately. An analysis of the possible excited states of the ^{69}Ga in this energy region shows that they are close to its α-emission energy (4.49 MeV). Besides, there are no well-established spin-parity states or reduced transition probabilities in this excitation energy region. Another possibility is the excitation of the ^{12}C ejectile, which has a 2^+ state with 4.44 MeV of excitation energy, which is compatible with the observed events. So, this state was added to the coupling scheme in the CRC calculations (with the spectroscopic amplitude set equal to 1). The results can be seen in Fig. 8, where the complete CRC calculation for the α-transfer process, including the inelastic channels and both recoil and ejectile excitations, is represented by the solid black line, which gives a good description of the experimental data. The contribution to this result of all the recoil excitations is represented by the dashed green line, and the contribution of the ejectile excitation by the dotted blue line. Very interesting results can be extracted from this figure. The theoretical lines reveal that the excitations of the recoil and the ejectile are energetically almost separated in the spectrum. A possible reason for this is the low α-emission energy of the ^{69}Ga (4.49 MeV) that hinders the excitation of its higher excitation states just at energies in which the ^{12}C starts being excited. Finally, as shown by the dashed red lines in Fig. 5, the α-transfer process has very little effect on both the quasielastic EF and the QEBD of the $^{16}O + ^{65}Cu$ system. This result is in agreement with numerous

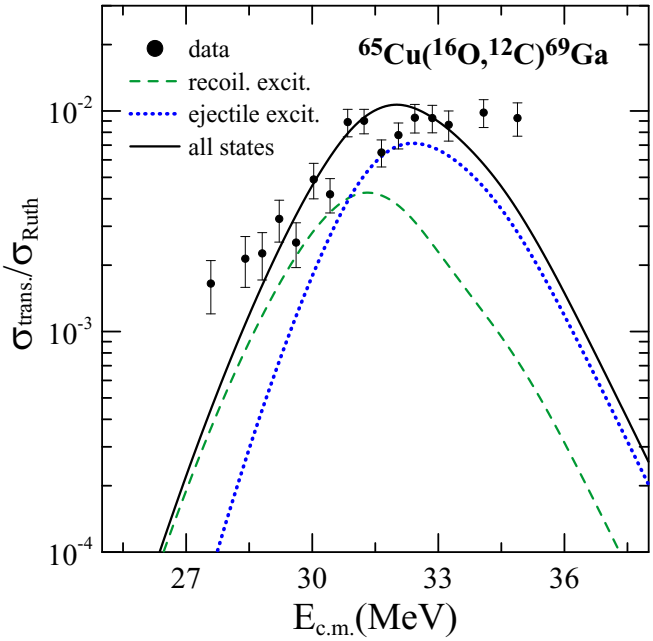


FIG. 8. Comparison of the experimental data and different theoretical excitation functions for the ^{16}O(^{65}Cu, ^{69}Ga)^{12}C reaction. The green dashed line corresponds to the sum of the cross section corresponding to excited states of the ^{69}Ga residual nucleus. The blue dotted line stands for the cross section when the ^{12}C ejectile was excited. The summed total cross section is represented by the solid black line.

neighboring systems studied in the literature, in which the transfer reactions are less important than the inelastic excitations in the reaction dynamics at energies around the Coulomb barrier [13,14,22,23,38,41–43].

D. Elastic scattering

In the previous sections, we investigated the roles of several reaction channels on reaction dynamics of the $^{16}\mathrm{O} + {}^{65}\mathrm{Cu}$ system as a function of the bombarding energy. To complete this study, we will now investigate how the same channels influence the angular distribution of elastically scattered nuclei. The same coupled-channel analysis will be made with an unpublished elastic scattering angular distribution for the $^{16}\mathrm{O} + {}^{65}\mathrm{Cu}$ system that was taken from Ref. [26]. In that work, the angular distributions were measured at energies well above the nominal Coulomb barrier of this system ($V_B = 39.8$ MeV, in laboratory framework). Among the energies they measured, we choose one of its lowest energies, $E_{\mathrm{LAB}} = 46.5$ MeV ($E_{\mathrm{c.m.}} = 37.3$ MeV), which corresponds to the highest energies measured in our work. This angular distribution covers the angular range between $\theta_{\mathrm{c.m.}} = 40^\circ$ and $\theta_{\mathrm{c.m.}} = 155^\circ$, approximately. Figure 9(a) shows the comparison of the CCC and experimental data for this bombarding energy. To put in evidence the reaction mechanism at forwarding angles, and the relative importance of the different channels, Fig. 9(b) presents the forward results also in a linear scale.

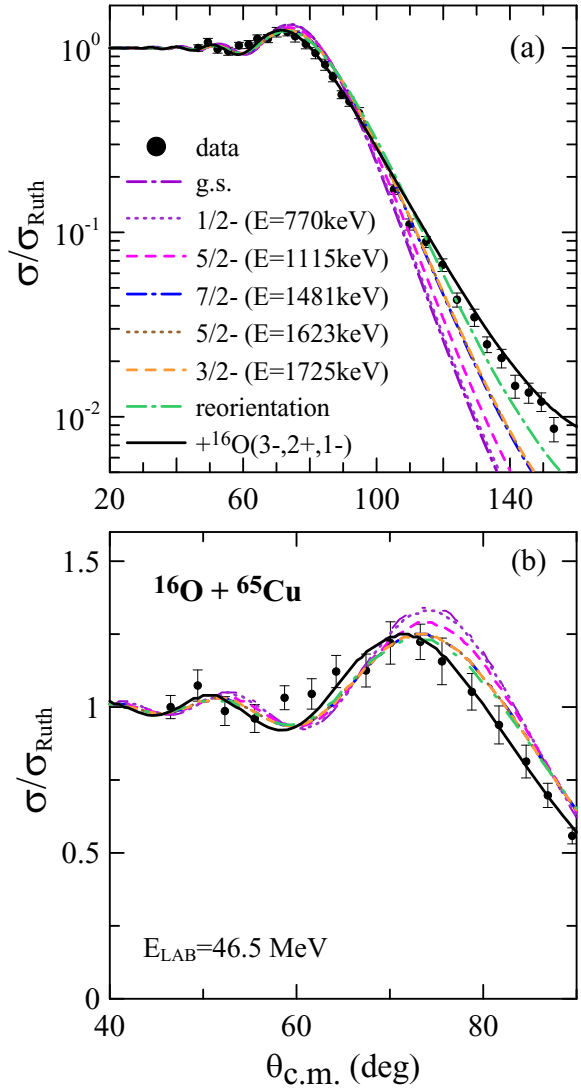


FIG. 9. (a) Angular distribution measured at $E_{\mathrm{LAB}} = 46.5$ MeV. The lines represent the different calculations (see text for further details). The vertical axis scale in logarithmic scale: (b) same as in panel (a), but the vertical axis is in linear scale.

As in Sec. III A, the theoretical results shown in Fig. 9 are the cumulative effect of the coupling of the inelastic channels that have been included one by one in the calculations. One can see a similar effect on the elastic scattering angular distribution as observed for the EF and QEBD described in detail in the previous sections. In Fig. 9, the uncoupled calculation (found state) is represented by the long-dash-dotted indigo line. One may observe by the dotted indigo line that the excitation of the first excited state of the ^{65}Cu, $1/2^-$, has little influence on the reaction mechanism. On the other hand, its second and third states, $5/2^-$ and $7/2^-$, represented in the figure by the dashed magenta and dash-dotted blue lines, respectively, have strong importance on the distribution of the scattered reaction flux, mainly the state $7/2^-$, which is the most relevant among all states investigated. One can also see in the figure that the second excited state $5/2^-$

($E = 1.62$ MeV) and the $3/2^-$ ($E = 1.72$ MeV) of the target have a very small effect on this reaction dynamics.

On the other hand, the dash-dotted green lines in Fig. 9 show that the reorientation of the ground state of the target has a striking influence on the redistribution of the incoming reaction flux, both at forward and backward angles. The same result has been obtained for the ^{63}Cu isotope in a previous work [22]. However, the inclusion of the α-transfer reaction does not affect appreciably the elastic scattering process and it is omitted in the figure. By comparing both panels in Fig. 9, it is interesting to observe that the overall effect of the inelastic channel couplings is to deviate the incoming flux from the forward angles to the backward ones, by lowering the Coulomb rainbow peak, at around $\theta_{\text{c.m.}} = 70^\circ$ and increasing the elastic cross section at backward angles.

Finally, we tested the effect on the elastic angular distribution of the same excited states of the ^{16}O investigated in a previous subsection. As shown by the solid black lines in Fig. 9, an excellent agreement with data was obtained in the entire angular region. However, this result was only obtained after inclusion in the calculations of states $^{16}O(2^+)$ and $^{16}O(1^-)$. Only the addition of the $^{16}O(3^-)$ state worsens the agreement of the calculation with data. That is, as in the EF, the opening of the states $^{16}O(2^+)$ and $^{16}O(1^-)$ are essential also for a good description of the elastic angular distribution in the system investigated. However, unlike the case of EF, the inclusion of the $^{16}O(2^-)$ state slightly worsens the agreement obtained.

IV. SUMMARY AND CONCLUSIONS

New experimental data are reported for the $^{16}O + ^{65}Cu$ system at energies around the Coulomb barrier, which has an odd-A nucleus target with large ground-state deformation. A high precision quasielastic excitation function for this system has been measured at the backward angle of $\theta_{\text{LAB}} = 161^\circ$, from which its quasielastic barrier distribution could be deduced. Besides, an excitation function for the α-stripping process have also been measured at the same angle and energies. In addition, an elastic angular distribution available in the literature, but not published yet, was also used in the theoretical analysis presented in this paper. All these new data obtained in this work were compared with the data of the neighboring $^{16}O + ^{63}Cu$ and $^{18}O + ^{63}Cu$ systems which we measured previously. It has been shown that their quasielastic excitation functions are similar, and all have a small structure at energies above the Coulomb barrier. On the other hand, the quasielastic barrier distribution of the $^{18}O + ^{63}Cu$ system is very different from the ones of the other two systems, indicating the determinant role of the ^{18}O nucleus in the reaction mechanism. In addition, the comparison of experimental α-stripping data of the $^{16}O + ^{63,65}Cu$ systems showed that the higher number of neutrons in the $f_{7/2}$ neutron subshell of the ^{65}Cu nucleus facilitates the α-transfer process at energies below the Coulomb barrier.

Parameter-free coupled-channel and coupled-reaction-channel calculations have been performed to investigate the relative contribution of each channel to the reaction mechanism of this system. In this sense, the goal of this theoretical approach was not to fit the data by varying potential parameters but rather to compare theoretical predictions with the data. The results of the theoretical analysis of this data indicated that the second and the third excited states ($5/2^-$ and $7/2^-$) of ^{65}Cu are quite important in a proper description of the experimental data, while the first excited state ($1/2^-$) has little influence. Besides, a striking influence of the reorientation of the ground-state target spin on the reaction dynamics was observed. These results are similar to those obtained earlier in the $^{16}O + ^{63}Cu$ system.

In the case of the $^{18}O + ^{63}Cu$ system, it was proved in a previous paper that the excitation of the ^{18}O nucleus plays an important role in the reaction dynamics of this system and produces that small structure in its quasielastic excitation function discussed above. Therefore, one would expect that the excitation of the ^{16}O could also be responsible for these structures in the other two systems. However, inclusion in the calculations of the conventional excited states $^{16}O(3^-)$ and $^{16}O(2^+)$did not produce large effects. As an alternative, excited states that are not usually introduced in the coupling schemes found in the literature, $^{16}O(1^-)$ and $^{16}O(2^-)$, were included in the complete CCC. These calculations are in good agreement with the data of the $^{16}O + ^{63}Cu$ and $^{16}O + ^{65}Cu$ systems, explaining even the small structures in the quasielastic excitation functions and quasielastic barrier distributions. Besides, the same CCC also provided a good description of the elastic angular distribution at 46.5 MeV. All these results in the three systems discussed in this paper show high coherence and reinforce the results obtained.

Finally, the inclusion of α-stripping channel in the coupling scheme has a small influence on the quasielastic cross sections. Nevertheless, the coupled-reaction-channel analysis of the α-stripping excitation function revealed very interesting details of this transfer process. As observed in Ref. [36], in the transfer of many nucleons, at energies around the Coulomb barrier, the excitation energy is distributed over many states and can spread to high excitation energies. This was confirmed by the $^{16}O(^{65}Cu, ^{69}Ga)^{12}C$ reaction studied in this paper, for which all excited states of the recoiling nucleus (^{69}Ga), up to its α-emission energy, cannot explain the excitation function data. Moreover, the PLF that emerges from this α-stripping reaction (^{12}C) is also left in its first (and high) excited state with high probability. The coupled-reaction-channel calculation including all these channels in the coupling scheme provides a good description for the experimental α-stripping excitation function.

ACKNOWLEDGMENTS

This work was financially supported by FAPESP, CNPq, CAPES, FAPERJ, and INCT-FNA (Instituto Nacional de Ciência e Tecnologia- Física Nuclear e Aplicações) (Proc. No. 464898/2014-5). One of the authors, E.C., is thankful for the financial support from CNPq (Proc. No. 305228/2015-3). We would like to thank the technical staff of Pelletron Laboratory for assisting in the maintenance and operation of the accelerator.

[1] W. Reisdorf, F. P. Hessberger, K. D. Hildenbrand, S. Hofmann, G. Munzenberg, K.-H. Schmidt, J. H. R. Schneider, W. F. W. Schneider, K. Sümmerer, G. Wirth, J. V. Kratz, and K. Schlitt, Phys. Rev. Lett. **49**, 1811 (1982).

[2] M. Beckerman, Rep. Prog. Phys. **51**, 1047 (1988).

[3] S. G. Steadman and M. J. Rhoades-Brown, Annu. Rev. Nucl. Sci. **36**, 649 (1986).

[4] C. H. Dasso, S. Landowne, and A. Winther, Nucl. Phys. A **405**, 381 (1983).

[5] R. G. Stokstad, Y. Eisen, S. Kaplanis, D. Pelte, U. Smilansky, and I. Tserruya, Phys. Rev. C **21**, 2427 (1980).

[6] D. E. DiGregorio, M. diTada, D. Abriola, M. Elgue, A. Etchegoyen, M. C. Etchegoyen, J. O. Fernández Niello, A. M. J. Ferrero, S. Gil, A. O. Macchiavelli, A. J. Pacheco, J. E. Testoni, P. R. Silveira Gomes, V. R. Vanin, R. L. Neto, E. Crema, and R. G. Stokstad, Phys. Rev. C **39**, 516 (1989).

[7] P. R. S. Gomes, I. C. Charret, R. Wanis, G. M. Sigaud, V. R. Vanin, R. Liguori Neto, D. Abriola, O. A. Capurro, D. E. DiGregorio, M. di Tada *et al.*, Phys. Rev. C **49**, 245 (1994).

[8] N. Rowley, G. R. Satchler, and P. H. Stelson, Phys. Lett. B **254**, 25 (1991).

[9] M. Dasgupta, D. J. Hinde, N. Rowley, and A. M. Stefanini, Annu. Rev. Nucl. Part. Sci. **48**, 401 (1998).

[10] H. Timmers, J. R. Leigh, M. Dasgupta, D. J. Hinde, R. C. Lemmon, J. C. Mein, C. R. Morton, J. O. Newton, and N. Rowley, Nucl. Phys. A **584**, 190 (1995).

[11] N. Rowley, H. Timmers, J. R. Leigh, M. Dasgupta, D. J. Hinde, J. C. Mein, C. R. Morton, and J. O. Newton, Phys. Lett. B **373**, 23 (1996).

[12] H. Timmers, D. Ackermann, S. Beghini, L. Corradi, J. H. He, G. Montagnoli, F. Scarlassara, A. M. Stefanini, and N. Rowley, Nucl. Phys. A **633**, 421 (1998).

[13] R. F. Simões, D. S. Monteiro, L. Kono, A. M. Jacob, J. M. B. Shorto, N. Added, and E. Crema, Phys. Lett. B **527**, 187 (2002).

[14] J. F. P. Huiza, E. Crema, D. S. Monteiro, J. M. B. Shorto, R. F. Simões, N. Added, and P. R. S. Gomes, Phys. Rev. C **75**, 064601 (2007).

[15] G. R. Satchler, Nucl. Phys. **45**, 197 (1963).

[16] G. R. Satchler and C. B. Fulmer, Phys. Lett. B **50**, 309 (1974).

[17] S. E. Hicks and M. T. McEllistrem, Nucl. Phys. A **468**, 372 (1987).

[18] V. Hnizdo, K. W. Kemper, and J. Szymakowski, Phys. Rev. Lett. **46**, 590 (1981).

[19] A. T. Rudchik, O. A. Momotyuk, V. A. Ziman, A. Budzanowski, A. Szczurek, I. Skwirczyńska, S. Kliczewski, and R. Siudak, Nucl. Phys. A **662**, 44 (2000).

[20] F. Videbk, P. R. Christensen, O. Hansen, and K. Ulbak, Nucl. Phys. A **256**, 301 (1976).

[21] V. V. Parkar, Sushil K. Sharma, R. Palit, S. Upadhyaya, A. Shrivastava, S. K. Pandit, K. Mahata, V. Jha, S. Santra, K. Ramachandran, T. N. Nag, P. K. Rath, B. Kanagalekar, and T. Trivedi, Phys. Rev. C **97**, 014607 (2018).

[22] J. M. B. Shorto, E. Crema, R. F. Simões, D. S. Monteiro, J. F. P. Huiza, N. Added, and P. R. S. Gomes, Phys. Rev. C **78**, 064610 (2008).

[23] E. Crema, V. A. B. Zagatto, J. M. B. Shorto, B. Paes, J. Lubian, R. F. Simões, D. S. Monteiro, J. F. P. Huiza, N. Added, M. C. Morais, and P. R. S. Gomes, Phys. Rev. C **98**, 044614 (2018).

[24] L. C. Chamon, B. V. Carlson, L. R. Gasques, D. Pereira, C. De Conti, M. A. G. Alvarez, M. S. Hussein, M. A. Candido Ribeiro, E. S. Rossi, Jr., and C. P. Silva, Phys. Rev. C **66**, 014610 (2002).

[25] M. A. G. Alvarez, L. C. Chamon, M. S. Hussein, D. Pereira, L. R. Gasques, E. S. Rossi Jr., and C. P. Silva, Nucl. Phys. A **723**, 93 (2003).

[26] L. C. Chamon, Experimental study on isotopic dependence on nuclear fusion and elastic scattering on $^{16,18}O + ^{63,65}Cu$ systems, Ph.D. thesis, University of São Paulo, Brazil, 1990 [http://www.teses.usp.br/teses/disponiveis/43/43131/tde-31082012-131325/pt-br.php]

[27] E. Crema, L. C. Chamon, and P. R. S. Gomes, Phys. Rev. C **72**, 034610 (2005).

[28] E. Crema, P. R. S. Gomes, and L. C. Chamon, Phys. Rev. C **75**, 037601 (2007).

[29] J. J. S. Alves, P. R. S. Gomes, J. Lubian, L. C. Chamon, D. Pereira, R. M. Anjos, E. S. Rossi Jr., C. P. Silva, M. A. G. Alvarez, G. P. A. Nobre, and L. R. Gasques, Nucl. Phys. A **748**, 59 (2005).

[30] A. Diaz-Torres and I. J. Thompson, Phys. Rev. C **65**, 024606 (2002).

[31] I. J. Thompson, Comput. Phys. Rep. **7**, 167 (1988).

[32] E. Browne and J. K. Tuli, Nucl. Data Sheets **111**, 2425 (2010).

[33] N. J. Stone, At. Data Nucl. Data Tables **90**, 75 (2005).

[34] D. R. Tilley, H. R. Weller, and C. M. Cheves, Nucl. Phys. A **564**, 1 (1993).

[35] T. Kibédi and R. H. Spear, At. Data Nucl. Data Tables **80**, 35 (2002).

[36] D. C. Rafferty, M. Dasgupta, D. J. Hinde, C. Simenel, E. C. Simpson, E. Williams, I. P. Carter, K. J. Cook, D. H. Luong, S. D. McNeil, K. Ramachandran, K. Vo-Phuoc, and A. Wakhle, Phys. Rev. C **94**, 024607 (2016).

[37] D. M. Brink, Phys. Lett. B **40**, 37 (1972).

[38] V. A. B. Zagatto, J. Lubian, L. R. Gasques, M. A. G. Alvarez, L. C. Chamon, J. R. B. Oliveira, J. A. Alcántara-Núñez, N. H. Medina, V. Scarduelli, A. Freitas, I. Padron, E. S. Rossi, Jr., and J. M. B. Shorto, Phys. Rev. C **95**, 064614 (2017).

[39] D. Kurath, Phys. Rev. C **7**, 1390 (1973).

[40] T. Motobayashi, I. Kohno, T. Ooi, and S. Nakajima, Nucl. Phys. A **331**, 193 (1979).

[41] N. Keeley, J. S. Lilley, J. X. Wei, M. Dasgupta, D. J. Hinde, J. R. Leigh, J. C. Mein, C. R. Morton, H. Timmers, N. Rowley, Nucl. Phys. A **628**, 1 (1998).

[42] J. F. P. Huiza, E. Crema, A. Barioni, D. S. Monteiro, J. M. B. Shorto, R. F. Simões, and P. R. S. Gomes, Phys. Rev. C **82**, 054603 (2010).

[43] V. A. B. Zagatto, F. Cappuzzello, J. Lubian, M. Cavallaro, R. Linares, D. Carbone, C. Agodi, A. Foti, S. Tudisco, J. S. Wang, J. R. B. Oliveira, and M. S. Hussein, Phys. Rev. C **97**, 054608 (2018).